Polymerization-induced spinodal decomposition of poly(ethylene-*co*-vinyl acetate)/methyl methacrylate mixture and the influence of incorporating poly(vinyl acetate) macromonomer*

Wenjie Chen, Sadayuki Kobayashi and Takashi Inoue†
Department of Organic and Polymeric Materials, Tokyo Institute of Technology, Ookayama, Meguro-ku, Tokyo 152, Japan

and Takashi Ohnaga
Central Research Laboratories, Kuraray, Sakazu, Kurashiki, Okayama 710, Japan

and Toshiaki Ougizawa
National Institute of Materials and Chemical Research, Polymer Processing Laboratory, Tsukuba, Ibaraki 305, Japan
(Received 6 December 1993; revised 1 February 1994)

The structural development during radical polymerization of a mixture of methyl methacrylate (MMA) and poly(ethylene-*co*-vinyl acetate) (EVA) was investigated by light scattering and optical microscopy. In the early stage of polymerization, the mixture of MMA/EVA was a single phase. As the polymerization of MMA proceeded, phase separation took place via spinodal decomposition (SD). This was supported by the characteristic change in light-scattering profile with reaction time. Analysis by the linearized and scaling theories showed that the reaction-induced phase separation behaviour was different from the familiar thermally induced SD during isothermal annealing after temperature jump. The scaling analysis showed that the final phase-separated structure may be formed by the interruption of a co-continuous percolation structure. Moreover, to investigate the effect of graft copolymer on SD, a poly(vinyl acetate) (PVAc) macromonomer with a methacrylate end-group was added to the MMA/EVA mixture to yield PMMA–PVAc graft copolymer during the polymerization. The incorporation of PVAc macromonomer increased the dominant wavenumber of the final frozen phase-separated structure (smaller periodic distance). The reasons seem to be that the concentration fluctuation growth is suppressed until the system reaches a deep quench depth at which the fluctuation should have a large wavenumber, and that the coarsening is retarded at the late stage by the graft copolymer formed *in situ*.

(Keywords: poly(ethylene-*co*-vinyl acetate); methyl methacrylate; spinodal decomposition)

INTRODUCTION

The spinodal decomposition induced by polymerization is typically demonstrated in an epoxy/poly(ether sulfone) system with a *LCST*(lower critical solution temperature)-type phase diagram. The binary mixture is homogeneous at curing temperature (below *LCST*). When the cure reaction proceeds, the system is thrust into a two-phase regime by the *LCST* depression caused by molecular weight increase and phase separation takes place via spinodal decomposition[1]. The reaction-induced spinodal decomposition yields a variety of two-phase structures: interconnected globule structure, isolated domain structure with uniform domain size, and bimodal domain structure, depending on the relative rates of the chemical reaction and the phase separation[1–3].

The chemical reaction in thermoset/thermoplastic systems is very complicated since it may involve chain extension, branching and crosslinking. In this paper, we deal with a simpler system: the radical polymerization of methyl methacrylate (MMA) in the presence of poly(ethylene-*co*-vinyl acetate) (EVA). In this system, the reaction is only the polymerization of MMA to form poly(methyl methacrylate) (PMMA). We also investigate the effect of graft copolymer formed *in situ* on the polymerization-induced phase separation. A poly(vinyl acetate) (PVAc) macromonomer with a methacrylate end-group is added to the MMA/EVA mixture to yield PMMA–PVAc graft copolymer during the polymerization. It is widely known that the presence of A–B graft copolymer at the interface in an A/B blend can reduce the interfacial tension and stabilize the fine dispersion[4].

* Presented in part at the 42nd Annual Meeting of the Society of Polymer Science, Japan and published as an abstract in *Polym. Prepr. Jap.* 1993, **42** (3), 1165

† To whom correspondence should be addressed

0032-3861/94/18/4015–07

Recent studies on isothermal phase demixing kinetics of a binary polymer blend showed that addition of a small amount of premade block copolymer could delay phase separation[5–7]. In the case of polymerization-induced phase separation, however, the situation might be different. We investigate polymerization-induced spinodal decomposition by time-resolved light scattering and discuss it on the basis of current understanding of spinodal decomposition.

EXPERIMENTAL

Poly(ethylene-*co*-vinyl acetate) (EVA) was supplied by Mitsui–du Pont Chemical Co. (EV-45LX; 46 wt% vinyl acetate content, $M_n = 2.75 \times 10^5$, $M_w/M_n = 1.9$ by gas permeation chromatography (g.p.c.)). Methyl methacrylate (MMA) and an initiator, α,α'-azobis(isobutyronitrile) (AIBN), were commercial products. They were used without further purification. Poly(vinyl acetate) (PVAc) macromonomer (MM) was synthesized following the method described in a previous paper[8]. Its chemical structure is

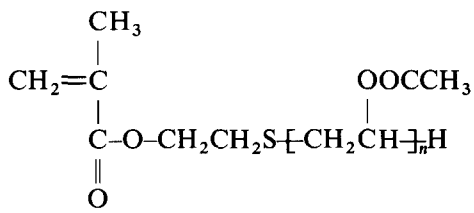

where the number-average degree of polymerization (n) was 35 by nuclear magnetic resonance (n.m.r.). EVA and AIBN were dissolved in MMA to make up a 20/80/0.2 (by weight) EVA/MMA/AIBN mixture. PVAc MM was added to the mixture at 1 part per hundred (phr) and 5 phr levels to prepare two mixtures with different PVAc MM content. The transparent mixtures thus obtained were sealed in a cell comprising two cover glasses and an aluminium spacer of thickness 0.1 mm with the aid of epoxy adhesive (*Figure 1a*).

Figure 1b shows the laser light-scattering apparatus used in this study. The sample cell was placed in a hot chamber kept at a constant temperature. The chamber was set horizontally on the light-scattering stage. The radiation from a He–Ne gas laser of wavelength 632.8 nm was applied vertically to the specimen. The goniometer trace of the scattered light was obtained under a V_v (parallel polarized) optical alignment. Thus the change in the light-scattering profile with time was recorded at appropriate intervals during isothermal polymerization. The scattering angle θ within the sample is related to the observed scattering angle, θ_{obs}, by

$$n \sin\theta = \sin\theta_{obs} \quad (1)$$

where n is the refractive index of the sample. The intensity of scattered light was corrected by multiplying by C_n:

$$C_n = n^2 \cos\theta/(1 - n^2 \sin^2\theta)^{1/2} \quad (2)$$

A light-scattering pattern was also taken by the photographic technique used by Stein and Rhodes[9].

The phase diagram of the MMA/EVA/PMMA ternary solution was measured by the cloud point method: a transparent mixture in a glass tube at an elevated temperature (80°C) was rapidly quenched to various temperatures and the change in turbidity with time was examined for 15 min by the naked eye. The cloud points thus measured had accuracy of ±1°C. The PMMA

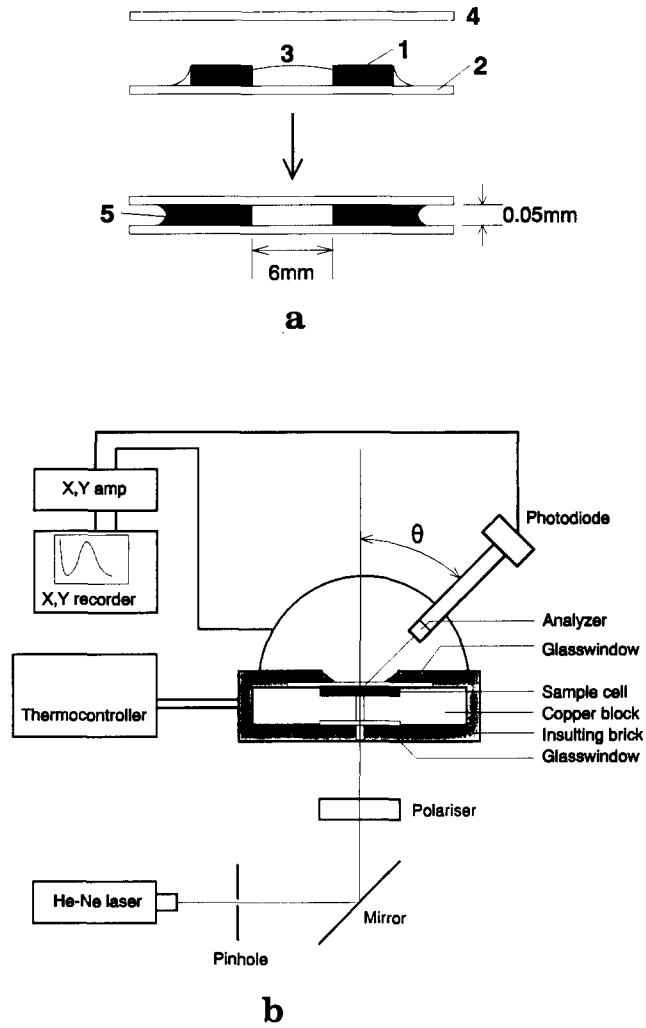

Figure 1 (a) Sample cell and (b) light-scattering apparatus. The monomer syrup was sealed in a cell as shown in (a); aluminium spacer **1** was preadhered on a thin glass plate (cover glass for microscopy) **2** by epoxy adhesive. A spacer **3** was filled with the syrup and the cell was sealed with another cover glass **4** by adding the adhesive **5**

used in this experiment was synthesized by bulk polymerization at 80°C, and its M_w and M_w/M_n by g.p.c. were 5.86×10^5 and 1.82, respectively. An inhibitor, *p-tert*-butylcatechol (0.1 wt%), was added to the ternary solution to prevent thermal polymerization of MMA during cloud point measurement.

MMA conversion was measured by differential scanning calorimetry (d.s.c.) (Du Pont 9000 Thermal Analyzer).

RESULTS AND DISCUSSION

Phase behaviour

Cloud point curves of PMMA/EVA/MMA ternary mixtures are shown in *Figure 2*, where m_0 indicates the weight fraction of MMA. Upper critical solution temperature (*UCST*)-type phase behaviour is seen. From these cloud point curves, one can draw a triangular phase diagram at a fixed temperature. In *Figure 3* is shown the diagram at 80°C. There is a small single-phase region in the diagram.

Since the EVA content was fixed at 20 wt%, the polymerization process can be described by the arrow in *Figure 3*. From the time–conversion curve at 80°C (*Figure 4*), the time variation of composition is shown by

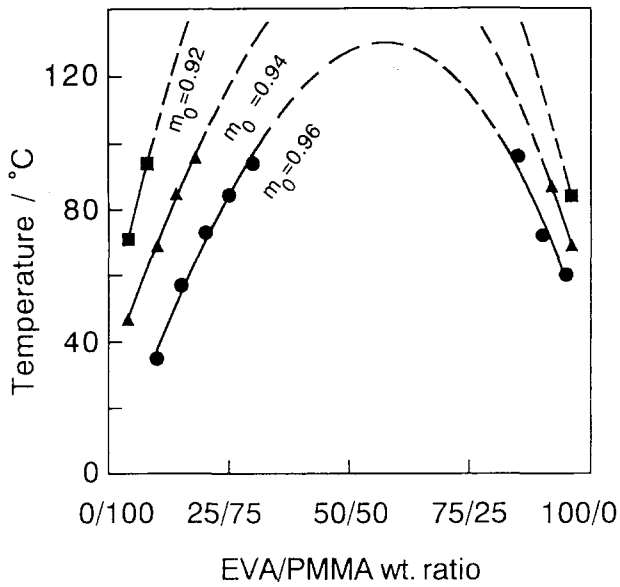

Figure 2 Cloud point curves in the PMMA/EVA/MMA ternary system; m_0, weight fraction of MMA

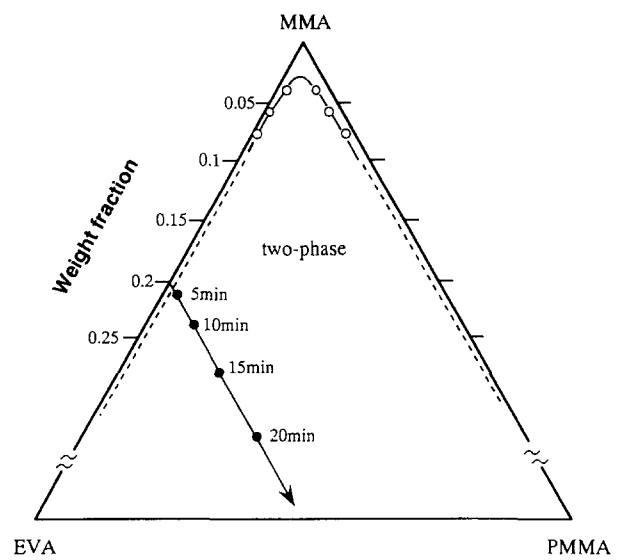

Figure 3 Triangular phase diagram of the MMA/EVA/PMMA system at 80°C. The points on the arrow show the composition–time relation for the 80/20/0.2 MMA/EVA/AIBN mixture during polymerization at 80°C

solid circles on the curve. In the triangular phase diagram, one can see that the system will be thrust into the two-phase regime when the polymerization proceeds to ≈2 wt% conversion level.

Morphology formation

Under the microscope, the system was homogeneous just after a temperature jump from room temperature to the polymerization temperature (80°C). After a certain time lag, a two-phase structure with low contrast appeared and the contrast became higher with polymerization time. In this time range, a ring pattern of the scattered light was detected and it became brighter with time, and then the ring diameter decreased at the late stage of polymerization. *Figure 5* shows a typical optical micrograph and light-scattering pattern of the specimen polymerized for 2 h. The micrograph clearly shows the uniform interdomain spacing and uniform domain size. It is consistent with the ring pattern. The regularly phase-separated structure is quite similar to that by isothermal spinodal decomposition.

The time-resolved light-scattering profiles are shown in *Figure 6*, where q is the scattering vector defined by

$$q=(4\pi/\lambda)\sin(\theta/2) \tag{3}$$

where λ is the wavelength of light in the specimen. A peak in the light-scattering profile appears after about 5 min and then increases continuously with time. Note that the peak position does not change up to 20 min. After the peak reaches a maximum, the peak position starts to shift toward a smaller angle as the polymerization progresses further. The peak shift continues up to 30 min and then the profile becomes invariant. From the peak angle q_m is calculated by equation (3). In *Figure 7* q_m is plotted as a function of reaction time t. The intensity at q_m, I_m, is similarly plotted in *Figure 7*. It is interesting that the q_m value remains constant for a very long time.

Combining the results in *Figures 7* and *4*, one can see that concentration fluctuation develops a periodic nature at about 2% conversion of MMA, the periodic distance ($2\pi/q_m$) remains essentially constant for a while (up to about 18% conversion) and then starts to increase, i.e. the structure coarsening proceeds; eventually the coarsening stops at 80% conversion.

Analysis by the linearized theory

It is interesting to check the applicability of the linearized theory of SD to the early stage of the reaction-induced SD. In the linearized theory the scattering intensity I grows exponentially

$$I(q,t)=I(q,0)\exp[2R(q)t] \tag{4}$$

where $R(q)$ is the amplification factor representing the growth rate of concentration fluctuation with q. $R(q)$ is described by

$$R(q)=-Mq^2\left(\frac{\partial^2 f}{\partial c^2}+2\kappa q^2\right) \tag{5}$$

where M is a translational diffusion constant, f is the free energy density of a homogeneous system at composition c, and κ is an energy gradient coefficient. Logarithmic

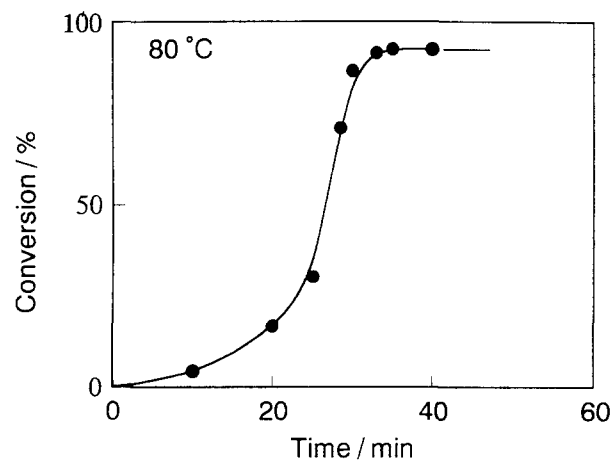

Figure 4 Time–conversion curve for the 80/20/0.2 MMA/EVA/AIBN mixture during polymerization at 80°C

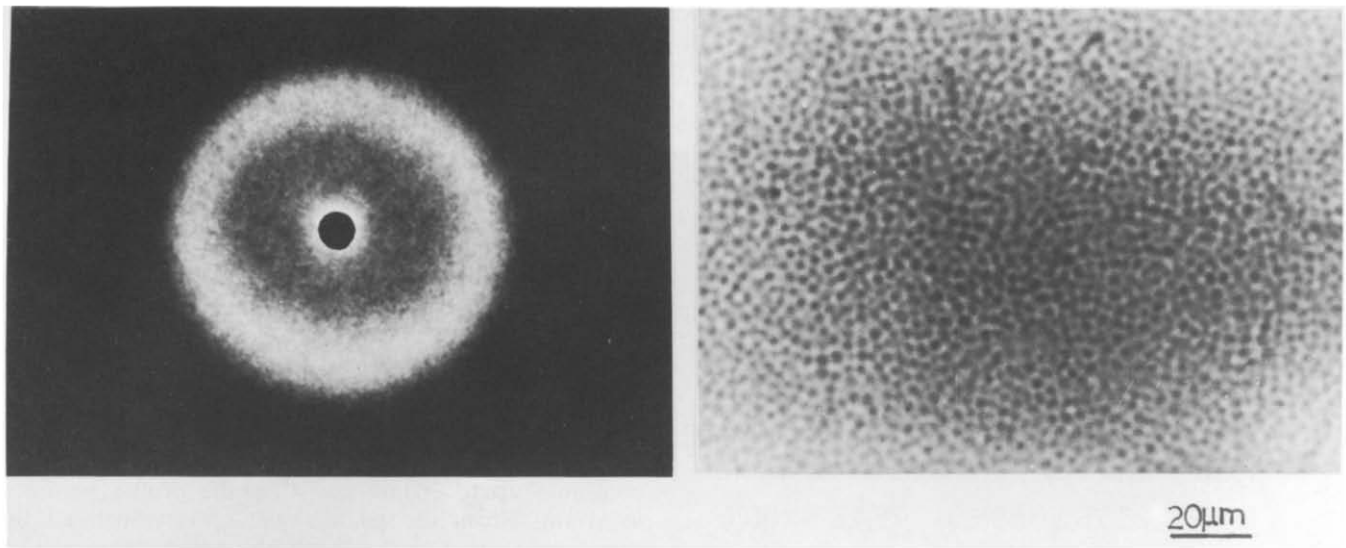

Figure 5 Light-scattering ring pattern (V_v) and the optical micrograph for the 80/20/0.2 MMA/EVA/AIBN mixture polymerized for 2 h at 80°C. The goniometer trace of the pattern is the curve at 32 min in *Figure 6*

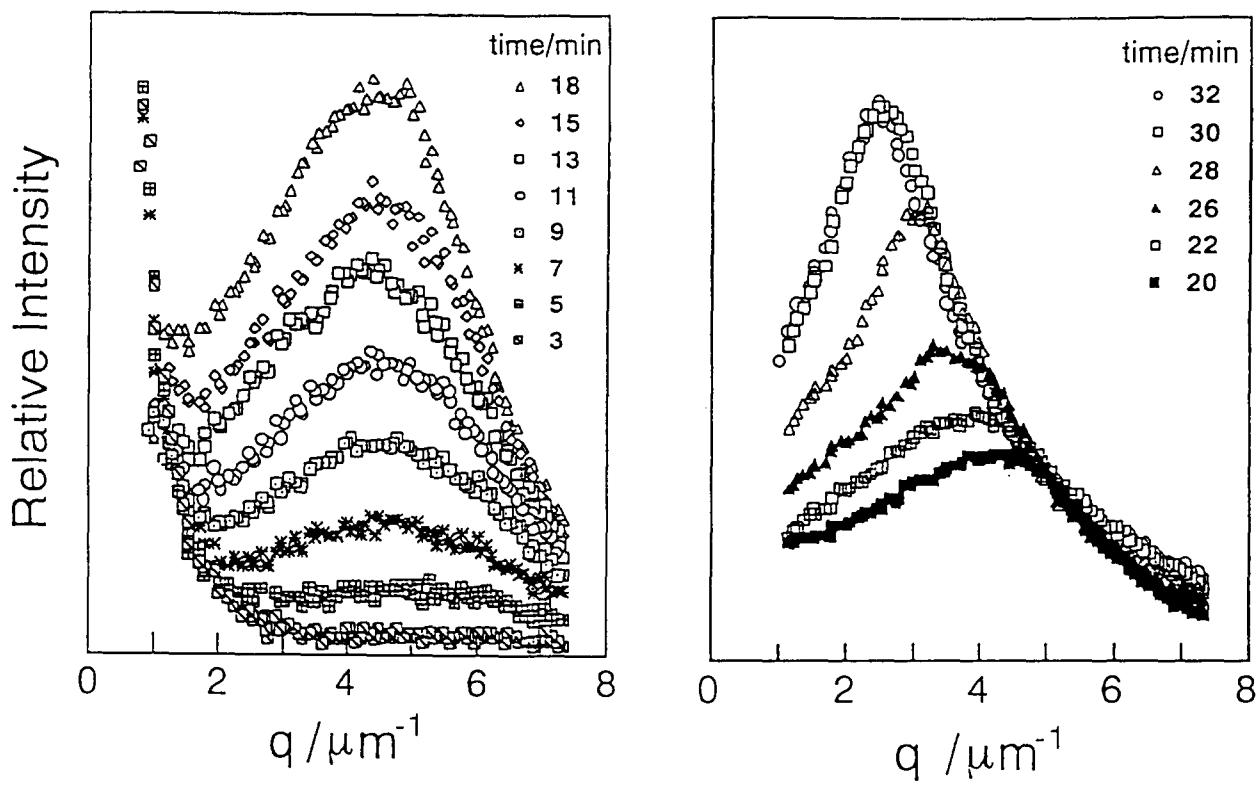

Figure 6 Time-resolved light-scattering profiles for 80/20/0.2 MMA/EVA/AIBN mixture polymerized at 80°C

plots of $I(q, t)$ at some selected wavenumbers are shown in *Figure 8*. At the early stage ($t < 8$ min), the linear regime is observed for all values of q. Note that, even after the deviation from linearity begins at $t > 8$ min, $q_m(t)$ still remains constant. This could be a very characteristic feature of SD induced by polymerization.

Using the values of $R(q)$ determined from the slopes of straight lines in the linear regime, the plot of $R(q)/q^2$ *versus* q^2 is given in *Figure 9*. As expected from equation (5), fairly straight lines are shown. The apparent diffusion coefficient, D_{app}, defined by

$$D_{app} = M \frac{\partial^2 f}{\partial c^2} \tag{6}$$

and the critical wavenumber $q_m(0)$ were obtained from intercepts on the x and y axes in *Figure 9*. Results are summarized in *Table 1*. Note that the above analyses are based on implicit assumptions: M, κ and $f(c)$ are constant (being independent of time). In general, these assumptions could not be satisfied in the reactive systems. However, the linear relationships in *Figures 8* and *9* may suggest that the assumptions are approximately true in the very early stage of the reaction-induced spinodal decomposition.

Scaling analysis for the late stage

The decrease in $q_m(t)$ accompanied by the increase in $I_m(t)$ with time at the late stage in *Figure 7* indicates the

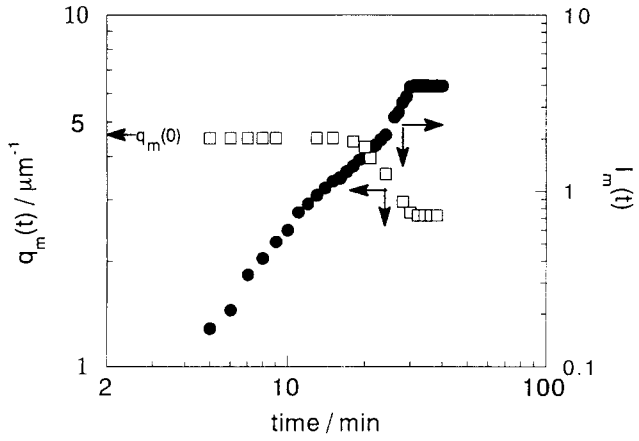

Figure 7 Plots of $q_m(t)$ and $I_m(t)$ *versus* time t for 80/20/0.2 MMA/EVA/AIBN at 80°C

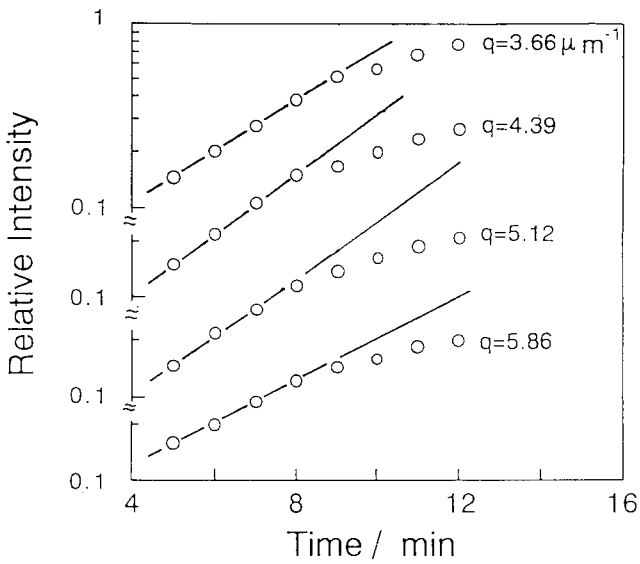

Figure 8 Variation of the logarithmic scattered intensity at various q with time t for 80/20/0.2 MMA/EVA/AIBN at 80°C

occurrence of coarsening. Time evolution of $q_m(t)$ and $I_m(t)$ is expressed by the power law:

$$q_m(t) = t^{-\alpha} \tag{7}$$

$$I_m(t) = t^{\beta} \tag{8}$$

The exponents α and β have been calculated for the SD in a simple binary system by many researchers. Langer, Baron and Miller (LBM) obtained the value of $\alpha = 0.21$ on the basis of non-linear statistical considerations[10]. Binder and Stauffer[11] considered the coalescence of cluster domains to get the values $\alpha = 1/3$ and $\beta = 1$. Lifshitz and Slyozov also predicted $\alpha = 1/3$ for solid mixtures according to the vaporization–condensation mechanism[12]. Siggia obtained $\alpha = 1/3$ for the early stage and $\alpha = 1$ for the intermediate stage (flow stage) by taking account of diffusion and hydrodynamic flow[13]. Thus various values for α and β have been reported depending on the coarsening mechanism. The exponents obtained from the slopes in the straight regime at the late stage, e.g. after about 20 min in *Figure 7*, are listed in *Table 1*. The values are close to those given by Siggia. This may imply that a percolation structure is initially formed and then transformed into clusters as seen in the final structure in *Figure 5*. It should be noted that this conclusion is only phenomenological, since in the reaction-induced SD many physical constants may change with time so that the basic assumptions might be violated.

In order to characterize the change of the phase-separated structure during polymerization, the time evolution of the scaled structure function was also investigated. Time evolution of a scattering profile $I(q, t)$ is expressed by[13]

$$I(q, t) \sim \langle \eta^2 \rangle q_m(t)^{-3} S(q(t)/q_m(t)) \tag{9}$$

where $S(q(t)/q_m(t))$ is the structure function, and $\langle \eta^2 \rangle$ is the mean-square fluctuation for the spatial variation of scattering contrast[14]:

$$\langle \eta^2 \rangle \sim \phi_1 \phi_2 (p_1 - p_2)^2 \tag{10}$$

ϕ_i and p_i indicate the volume fraction and the polarizability of phase i, respectively. Then the experimental scaled structure function is obtained by

$$F(X, t) = q_m(t)^3 I(q, t) \tag{11}$$

with $X = q(t)/q_m(t)$. From equations (9) and (11), $F(x, t)$ is related to $S(x)$ by

$$F(X, t) \sim \langle \eta^2 \rangle S(X) \tag{12}$$

Furukawa[16] proposed the scaled structure function as

$$S(X) = \frac{X^2}{r/2 + X^{2+r}} \tag{13}$$

and pointed out that

$$r = d + 1 \quad \text{for cluster regime}$$

and

$$r = 2d \quad \text{for percolation regime}$$

where d is the dimensionality of the system.

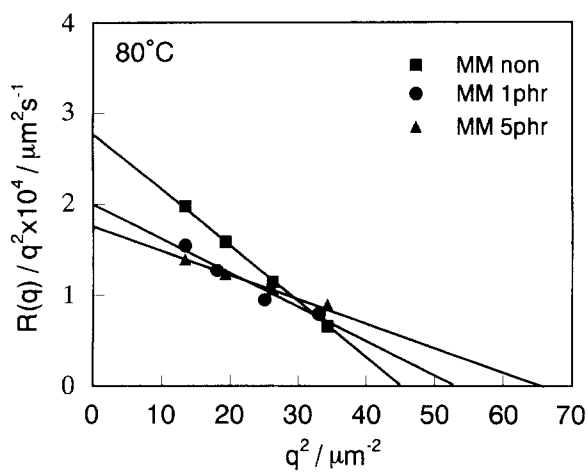

Figure 9 Plots of $E(q)/q^2$ *versus* q^2 for various MM content

Table 1 Kinetic parameters describing the polymerization-induced SD

MM content (phr)	$-D_{app} \times 10^{12}$ (cm^2 s^{-1})	$q_m(0)$ (μm^{-1})	α	β	$\Delta\Lambda_m/\Delta_t$ (μm min^{-1})
0	2.7	4.74	1.07	2.68	0.104
1	2.0	5.10	0.84	2.24	0.032
5	1.7	5.70	0.83	2.24	0.025

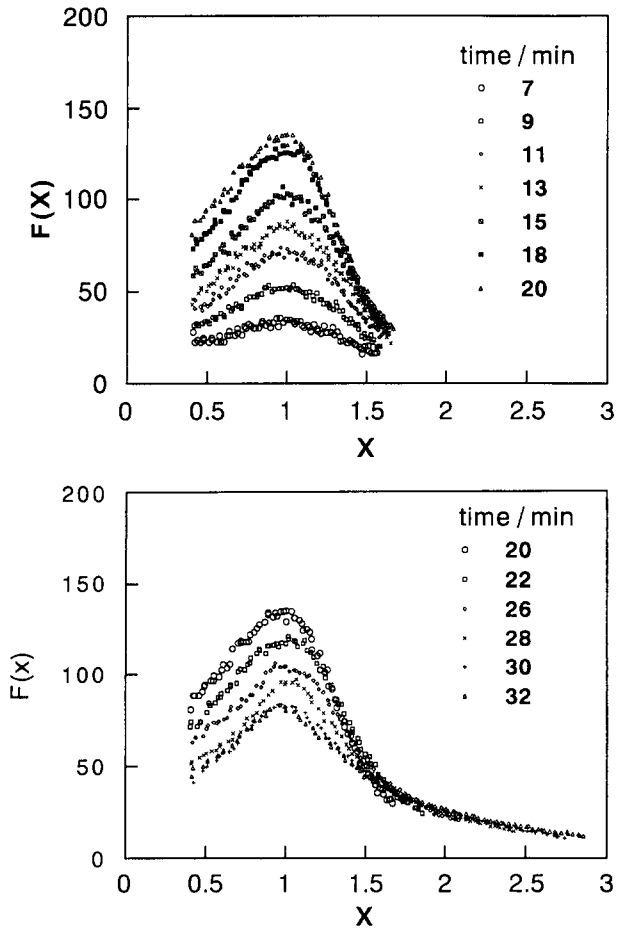

Figure 10 Time variation of scaled structure factor for 80/20/0.2 MMA/EVA/AIBN polymerized at 80°C

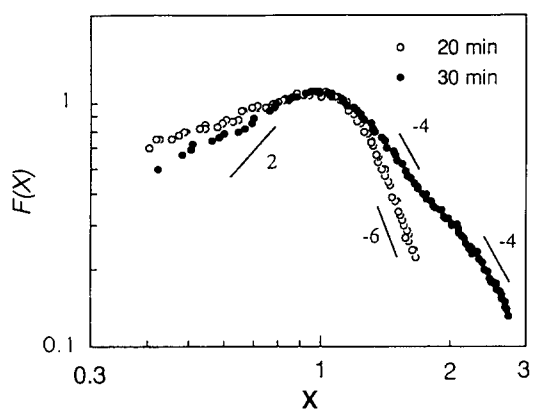

Figure 11 Scale structure factor at $t=20$ (○) and 30 (●) min for 80/20/0.2 MMA/EVA/AIBN at 80°C

Figure 10 shows the time variation of $F(X, t)$ calculated from the result in *Figure 6*. Up to 20 min, $F(X, t)$ increases continuously with time. This seems to be due primarily to the increase in composition difference between two phases; $F(x, t)$ sharpens with time, indicating the formation of a better defined structure. When $t > 20$ min, $F(x, t)$ decreases in intensity, and becomes broader continuously with time. This implies that the structure factor $S(X, t)$ broadens during this stage. The decrease of $F(x, t)$ with time might be derived from the decrease of $\langle \eta^2 \rangle$ and/or the broadening of $S(X, t)$[17]. In equation (10) $\phi_1\phi_2$ has a maximum value when $\phi_1 = \phi_2 = 0.5$; i.e. the larger the deviation from symmetry, the smaller is the product of $\phi_1\phi_2$. When the system reaches ≈20 wt% conversion, ϕ_1 and ϕ_2 could be approximately equal and further polymerization would lead the deviation from symmetry of composition (see *Figure 3*). Thus a decrease of $\langle \eta^2 \rangle$ with time will occur when the decrease of $\phi_1\phi_2$ prevails over the increase of $(p_1 - p_2)^2$.

In *Figure 11* are shown the double logarithmic plots of the reduced scaled structure function $F(X, t) = F(X,t)/F(1, t)$ for $t = 20$ min and $t = 32$ min. A slope of the plot for $t = 20$ min in the X range $1.4 < X < 1.6$ is approximated by $F(X, t) \sim X^{-6}$. According to equation (13), this slope is expected for bicontinuous percolated networks. On the other hand, $F(X, t)$ for $t = 32$ min is described by $F(X, t) \sim X^{-4}$ (for $1.4 < X < 1.6$) reflecting the cluster structure and $F(X, t) \sim X^{-4}$ (for $X > 2.2$) suggesting Porod's regime. Thus one can see that the broadening of the structure factor at $t > 20$ min is associated with the transformation from a percolation to a cluster structure.

Effect of PVAc macromonomer

Incorporating PVAc MM, there was no qualitative change in the time-variation light-scattering profile. The results by the linearized theory are shown in *Figure 9* and *Table 1*. One can see that $q_m(0)$ becomes larger and D_{app} becomes smaller as the MM content increases. Time variations of $q_m(t)$ and $I_m(t)$ are shown in *Figures 12* and *13*. The exponents α and β were obtained using

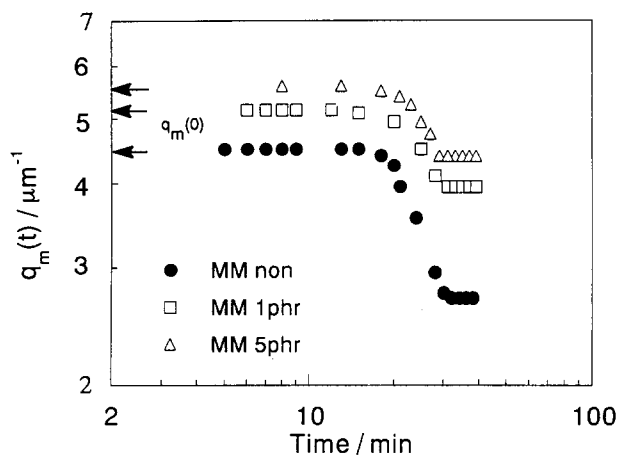

Figure 12 Time variation of $q_m(t)$ for 80/20/0.2 MMA/EVA/AIBN at 80°C for various MM content

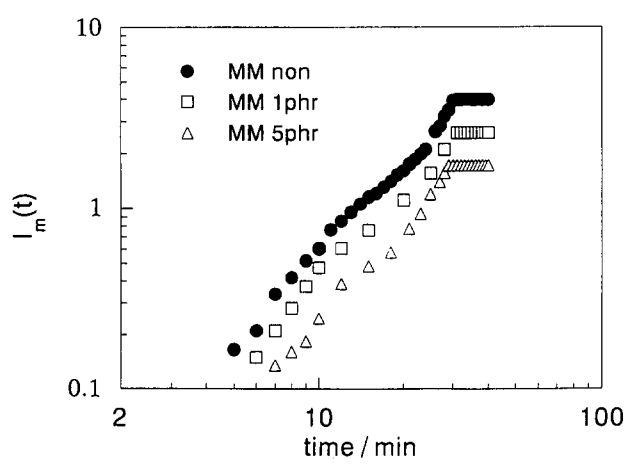

Figure 13 Time variation of $I_m(t)$ for 80/20/0.2 MMA/EVA/AIBN at 80°C for various MM content

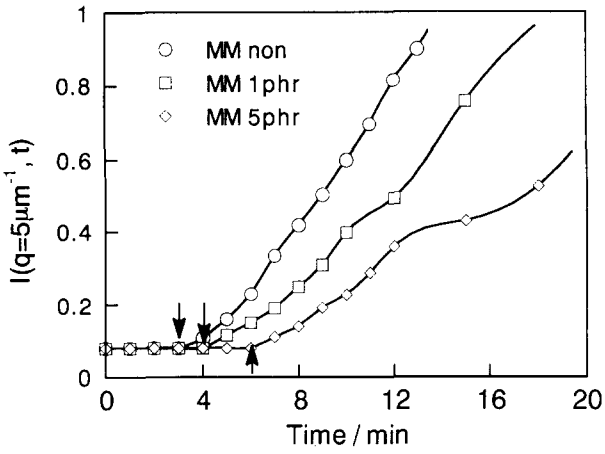

Figure 14 The intensity of scattered light at $q = 5\,\mu m^{-1}$ as a function of time for 80/20/0.2 MMA/EVA/AIBN at 80°C and various MM content. The arrows indicate the onset of the scattering intensity increase

equations (7) and (8) and are summarized in *Table 1*. The values of α and β become smaller with the increase in MM content. This means that the coarsening mechanism is affected by the formation of graft copolymer during polymerization. To characterize the coarsening rate, a velocity constant $\Delta\Lambda_m/\Delta t$ was defined as the time variation of $\Lambda_m(t)$ ($\Lambda_m(t) = 2\pi/q_m(t)$ being the periodic distance) in a limited time range 20 min $< t <$ 30 min. The results are shown in *Table 1*. One can see that the higher the MM, the slower is the rate. This result may be discussed according to Siggia's equation[13],

$$\Lambda_m(t) \sim (\sigma/\eta)t \qquad (14)$$

where σ is the interfacial tension and η the viscosity. The velocity of coarsening becomes slower if the interfacial tension decreases and this may be attained in the polymerizing mixture by the formation of PMMA–PVAc graft copolymer.

The reason why q_m becomes larger when MM is added is not obvious at present. However, if the scattering intensity at a fixed scattering angle ($q = 5\,\mu m^{-1}$) is plotted as a function of polymerization time (*Figure 14*), one sees that the onset of increase in the scattering intensity is delayed by MM addition, i.e. the occurrence of phase separation is suppressed by the increase of MM content. This probably suggests that the evolution of concentration fluctuation is suppressed by the existence of PMMA–PVAc graft copolymer at low quench depth and the fluctuation develops only when a high quench depth is attained. At the high quench depth, $q_m(0)$ should be large.

CONCLUSIONS

We have found that the phase separation during polymerization of MMA in the presence of EVA can be interpreted in terms of a phase separation scheme based on SD, which is induced by the increase of PMMA content in the mixture. This phase separation behaviour is different from the ordinary isothermal SD. The final phase-separation structure may be formed by interruption of a co-continuous percolation structure to the cluster structure.

Incorporation of PVAc macromonomer into the MMA/EVA mixture to provide *in situ* formation of PMMA–PVAc graft copolymer during the polymerization process resulted in a reduced periodic distance phase-separated structure. The reduction seems to be caused by two effects: (i) the growth of concentration fluctuation with short wavelength at the early stage, and (ii) retardation of coarsening at the late stage.

REFERENCES

1 Yamanaka, K. and Inoue, T. *J. Mater. Sci.* 1990, **25**, 241
2 Yamanaka, K., Takagi, Y. and Inoue, T. *Polymer* 1989, **60**, 1839
3 Yamanaka, K. and Inoue, T. *Polymer* 1989, **30**, 662
4 Paul, D. R. and Newman, S. (eds) 'Polymer Blends', Academic Press, New York, 1978
5 Roe, R. J. and Kuo, C. M. *Macromolecules* 1990, **23**, 4635
6 Park, D. W. and Roe, R. J. *Macromolecules* 1991, **24**, 5324
7 Hashimoto, T. and Izumitani, T. *Macromolecules* 1993, **26**, 3631
8 Ohnaga, T. and Sato, T. *Polym. Prepr. Jpn.* 1990, **39** (7), 1991
9 Stein, R. S. and Rhodes, M. B. *J. Appl. Phys.* 1960, **31**, 1873
10 Langer, J. S., Baron, M. and Miller, H. D. *Phys. Rev.* (*A*) 1975, **11**, 1417
11 Binder, K. and Stauffer, D. *Phys. Rev. Lett.* 1973, **33**, 1006
12 Lifshitz, I. M. and Slyozov, V. V. *J. Phys. Chem. Solids* 1961, **19**, 35
13 Siggia, E. D. *Phys. Rev.* (*A*) 1979, **20** (2), 595
14 Hashimoto, T., Itakura, M. and Hasegawa, H. *J. Chem. Phys.* 1986, **85** (10), 6118
15 Koberstein, J., Russell, T. P. and Stein, R. S. *J. Polym. Sci. Polym. Phys. Edn* 1979, **17**, 1719
16 Furukawa, H. *Physica* (*A*) 1984, **123**, 497
17 Takenaka, M., Izumitani, T. and Hashimoto, T. *J. Chem. Phys.* 1993, **98** (4), 3528